Aquaporin 1 regulates GTP-induced rapid gating of water in secretory vesicles

Sang-Joon Cho*, A. K. M. Abdus Sattar*, Eun-Hwan Jeong*, Mylan Satchi*, Jin Ah Cho*, Sudhansu Dash*, Mary Sue Mayes†, Marvin H. Stromer†, and Bhanu P. Jena*‡

*Departments of Physiology and Pharmacology, Wayne State University School of Medicine, Detroit, MI 48201; and †Departments of Animal Science, Biochemistry, and Biophysics, Iowa State University, Ames, IA 50011

Communicated by Robert W. Berliner, Yale University School of Medicine, New Haven, CT, February 11, 2002 (received for review January 7, 2002)

The swelling of secretory vesicles has been implicated in exocytosis, but the underlying mechanism of vesicle swelling remains largely unknown. Zymogen granules (ZGs), the membrane-bound secretory vesicles in exocrine pancreas, swell in response to GTP mediated by a $G_{\alpha i3}$ protein. Evidence is presented here that the water channel aquaporin-1 (AQP1) is present in the ZG membrane and participates in rapid GTP-induced vesicular water gating and swelling. Isolated ZGs exhibit low basal water permeability. However, exposure of granules to GTP results in a marked potentiation of water entry. Treatment of ZGs with the known water channel inhibitor Hg^{2+} is accompanied by a reversible loss in both the basal and GTP-stimulatable water entry and vesicle swelling. Introduction of AQP1-specific antibody raised against the carboxyl-terminal domain of AQP1 blocks GTP-stimulable swelling of vesicles. Our results demonstrate that AQP1 associated at the ZG membrane is involved in basal as well as GTP-induced rapid gating of water in ZGs of the exocrine pancreas.

zymogen granule | atomic force microscopy

Secretory vesicle swelling is critical for exocytosis (1–4); however, the underlying mechanism of vesicle swelling is largely unknown. In mast cells, an increase in secretory vesicle volume after stimulation of secretion has been suggested from electrophysiological measurements (5). The requirement of osmotic force in the fusion of phospholipid vesicles with a membrane bilayer also has been demonstrated (6). Isolated zymogen granules (ZGs), the membrane-bound secretory vesicles in exocrine pancreas and parotid glands, possess Cl^- and ATP-sensitive, K^+-selective ion channels at the vesicle membrane, whose activities are implicated in vesicle swelling (7–15). Additionally, secretion of ZG contents in permeabilized pancreatic acinar cells requires the presence of both K^+ and Cl^- ions (3). *In vitro* ZG-pancreatic plasma membrane fusion assays demonstrate potentiation of fusion in the presence of GTP and NaF (ref. 16; unpublished observation). Heterotrimeric Gαi3 protein has been implicated in the regulation of both K^+ and Cl^- ion channels in a number of tissues (17–21). Analogous to the regulation of K^+ and Cl^- ion channels at the cell membrane, the regulation of K^+ and Cl^- ion channels at the ZG membrane by a Gαi protein is suggested (22). Isolated ZGs from exocrine pancreas swell rapidly in response to GTP and NaF (22). These studies suggest the involvement of rapid water entry into ZGs after exposure to GTP. As opposed to osmotic swelling, membrane-associated water channels called aquaporins have been implicated in rapid volume changes in cells (8, 11) and intracellular vesicles (7, 10). Therefore, the likely mechanism of ZG swelling by means of possible water channels at the ZG membrane was explored. This study demonstrates the presence of aquaporin-1 (AQP1) in ZG membranes and its participation in GTP-mediated vesicle water entry and swelling.

Materials and Methods

Cell Fraction Preparation for Immunoblot. Rat pancreatic fractions were prepared and their purity was determined as described (12, 13, 23). Salt and detergent treatment of isolated ZG membrane preparations were performed at 4°C for 30 min. After treatment, supernatant and particulate fractions were separated by centrifugation of the reaction mixture at 4°C for 1 h at 200,000 × *g*.

Immunoblot Analysis of Cell Fractions. Immunoblot analysis was performed on pancreatic fractions prepared as described (10). Protein in pancreatic fractions was estimated by the Bradford method (14). Pancreatic fractions were boiled in Laemmli, reducing sample preparation buffer (15) for 5 min. Equal loads of protein were resolved in a 12.5% SDS/polyacrylamide gel, followed by electrotransfer to 0.2-μm nitrocellulose sheets. The nitrocellulose was incubated for 1 h at room temperature in blocking buffer (5% nonfat milk in PBS containing 0.1% Triton X-100 and 0.02% NaN_3) and immunoblotted for 2 h at room temperature with either affinity-purified B-CHIP (AQP1) antibody raised against the holoprotein (11), a gift from B. Baum and M. A. Knepper (National Institutes of Health), or monoclonal vesicle-associated membrane protein (VAMP) antibody recognizing VAMP1 and VAMP2 from StressGen Biotechnologies (Victoria, Canada). Both primary antibodies were used at a dilution of 1:1,000 in blocking buffer. The immunoblotted nitrocellulose sheets were washed in PBS containing 0.1% Triton X-100 and 0.002% NaN_3, before incubation, for 1 h at room temperature in horseradish peroxidase-conjugated secondary antibody at a dilution of 1:2,000 in blocking buffer. The immunoblots were washed in PBS containing 0.1% Triton X-100 and 0.02% NaN_3 and processed for enhanced chemiluminescence and exposure to X-Omat-AR film. The exposed films then were developed and photographed.

Immunoelectron Microscopy of ZGs. Sections were prepared from rat pancreatic lobules embedded in unicryl, and immunogold labeling was performed (24) by using an antibody raised to the carboxyl terminus of AQP1. Labeling and visualization involved blocking steps and the use of 10 nm of gold-conjugated anti-rabbit antibody.

Atomic Force Microscopy in the Measurement of ZG Dynamics. Isolated ZG suspensions in 125 mM KCl-Mes buffer, pH 6.5 (25 mM KCl/100 mM 2-*N*-morpholinoethanesulfonic acid) were plated on Cell-Tak-coated glass coverslips. Ten minutes after plating, the coverslips were placed in a fluid chamber and washed with the KCl-Mes buffer to remove unattached granules, before imaging the attached ZG in KCl-Mes buffer or water, in

Abbreviations: ZG, zymogen granule; AQP1, aquaporin-1; SLO, streptolysin-O; VAMP, vesicle-associated membrane protein.

‡To whom reprint requests should be addressed at: Department of Physiology and Pharmacology, Wayne State University School of Medicine, 5239 Gordon Scott Hall, 540E Canfield Avenue, Detroit, MI 48201-1928. E-mail: bjena@med.wayne.edu.

The publication costs of this article were defrayed in part by page charge payment. This article must therefore be hereby marked "*advertisement*" in accordance with 18 U.S.C. §1734 solely to indicate this fact.

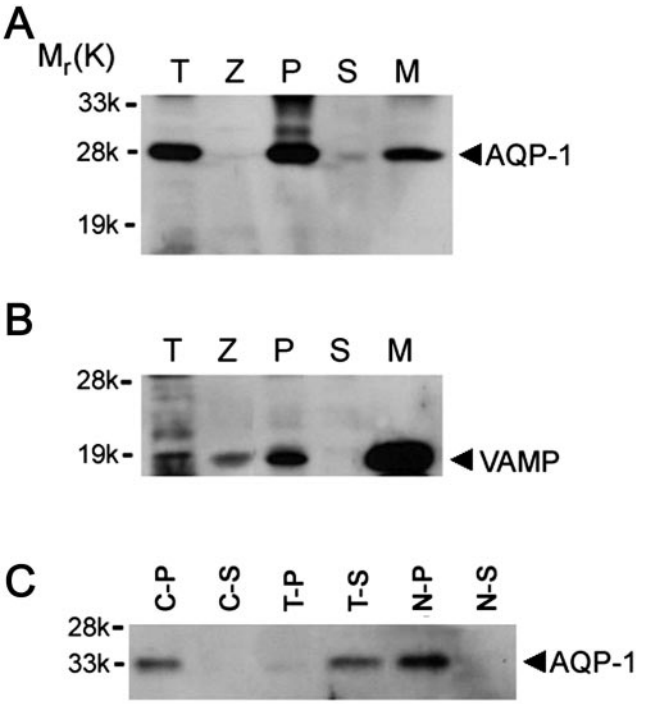

Fig. 1. AQP1 immunoreactivity is tightly associated with the ZG membrane fraction. Twenty micrograms of protein from each of the rat pancreatic fractions, total homogenate (T), zymogen granule (Z), 200,000 × *g* particulate (P), and supernatant (S) from total homogenates, and zymogen granule membrane (M), was resolved by using 12.5% SDS/PAGE. The resolved proteins in each fraction were electrotransferred to nitrocellulose membrane and immunoblotted with AQP1 and VAMP-specific antibodies. The 28-kDa AQP1 immunoreactivity is associated with the M fraction (*A*). The purity of isolated Z is demonstrated by the enriched presence of VAMP in the M fraction (*B*). ZGs are membrane-bound secretory vesicles packed with secretory proteins. The membrane fraction constitutes <1% of total granular proteins. Thus, very little AQP1 and VAMP immunoreactivity is detected in total granules, compared with severalfold enrichment in the granule membrane fraction. Affinity of AQP1 association with M was examined further by exposing 10 μg of granule membrane protein to buffer, salt, and detergent (*C*). After treatment of the granule membrane, the particulate and supernatant fractions were separated by centrifugation at 200,000 × *g*. Examination of particulate (C-P) and supernatant (C-S) fractions prepared after PBS treatment, treatment with 1% Triton X-100 in PBS (T-P, T-S), or with 1 M KCl (N-P, N-S) demonstrates specific and tight association of AQP1 immunoreactivity with M. Exposure of the M to PBS or 1 M KCl failed to dislodge the AQP1 immunoreactivity; however, the nonionic detergent Triton X-100 was able to dissociate AQP1 from the granule membrane.

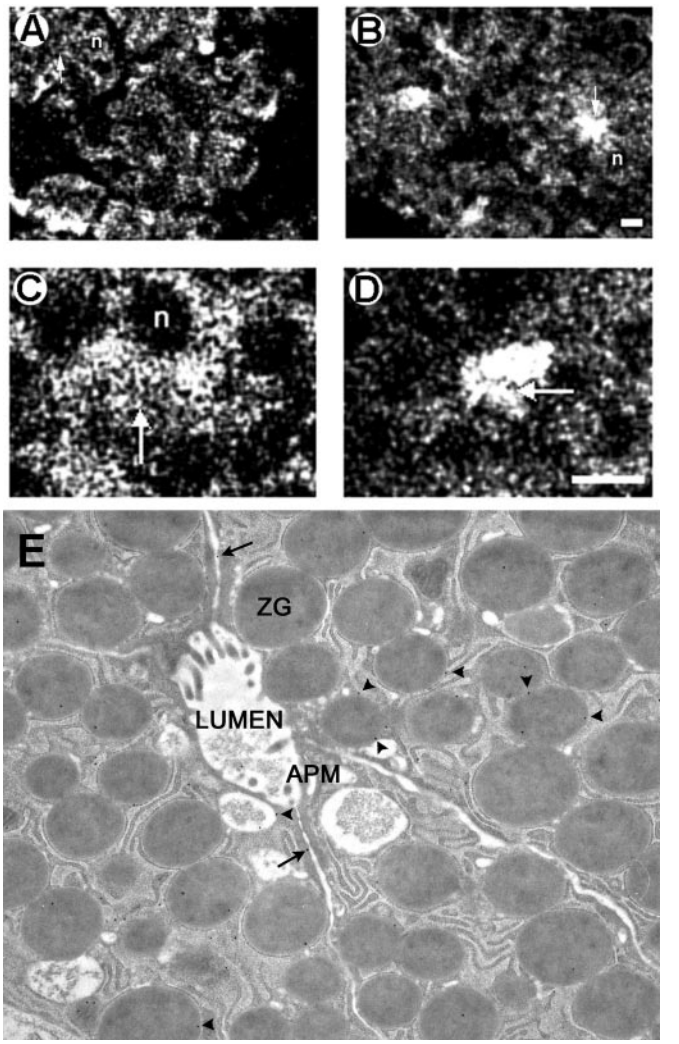

Fig. 2. AQP1 is associated with ZGs in pancreatic acinar cells. (*A–D*) AQP1 immunofluorescent confocal microscopy on stimulated and resting pancreatic lobules. Pancreatic lobules incubated for 1 h at 37°C in the absence (resting) or presence (stimulated) of the secretagogue, carbamylcholine (1×10^{-5} M). A 4-fold increase in amylase secretion from stimulated pancreatic lobules over resting was observed (data not shown). After incubation, the lobules were fixed, cryosectioned, and processed for immunofluorescent confocal microscopy. Confocal images of AQP1-immunostained pancreatic tissue in resting (*A* and *C*) and stimulated (*B* and *D*) states indicate association of AQP1 with ZG and its possible involvement in secretion. In resting acinar cells, AQP1 appears distributed throughout the cell including the apical region (arrow). The nuclei (n) located at the basolateral end of pancreatic acinar cells are devoid of AQP1-specific immunostaining. After stimulation of secretion, much of the AQP1 immunoreactivity is localized at the apical region of pancreatic acinar cells, where secretion is known to occur. (Bar = 10 μm.) (*E*) Immunogold electron microscopic (10-nm particles) localization of AQP1 to ZG (arrowheads). Note some AQP1 associated with the cell plasma membrane (arrow). (Magnification: ×57,000.)

the presence or absence of various concentrations of GTP, 25 μM $HgCl_2$, and 100 μM 2-mercaptoethanol. AQP1 antibody raised against the carboxyl-terminal domain of AQP1 (Santa Cruz Biotechnology) was introduced into the ZG lumen by incubating the ZG at 4°C for 5 min in KCl-Mes buffer containing streptolysin-O (SLO) and the antibody or vehicle, followed by a 2-min incubation at 30°C and three washes in ice-cold 125 mM KCl-Mes buffer, pH 6.5. At 4°C, the SLO binds to the cholesterol molecule at the ZG membrane, making approximately 14-nm holes at 30°C, which allow antibodies (≈8 nm) to enter the ZG. Washing ZG with ice-cold 125 mM KCl-Mes buffer reseals the holes and removes ZG-associated SLO. After incubation, the ZGs containing AQP1 antibody or the vehicle were washed and imaged in the presence of 40 μM GTP. ZG imaging and dynamics were performed by using the Nanoscope IIIa, an atomic force microscopic from Digital Instruments (Santa Barbara, CA). ZGs were imaged both in the "contact" and "tapping" mode in fluid (25, 26). However, all images presented in this manuscript were obtained in the "tapping" mode in fluid, using silicon nitride tips with a spring constant of 0.06 $M \cdot m^{-1}$ and an imaging force of less than 200 nN. Images were obtained at line frequencies of 2 Hz, with 512 lines per image and constant image gains. Time-dependent (resolution in seconds), morphological changes in ZG were obtained by using section analysis. Topographical dimensions of ZG were analyzed with the software NANOSCOPE (R) IIIA 4.43r8 supplied by Digital Instruments.

Measurement of Tritiated Water Entry. Isolated ZGs in 100 mM Mes buffer (pH 6.5) containing 50,000 cpm of tritiated water

PHYSIOLOGY

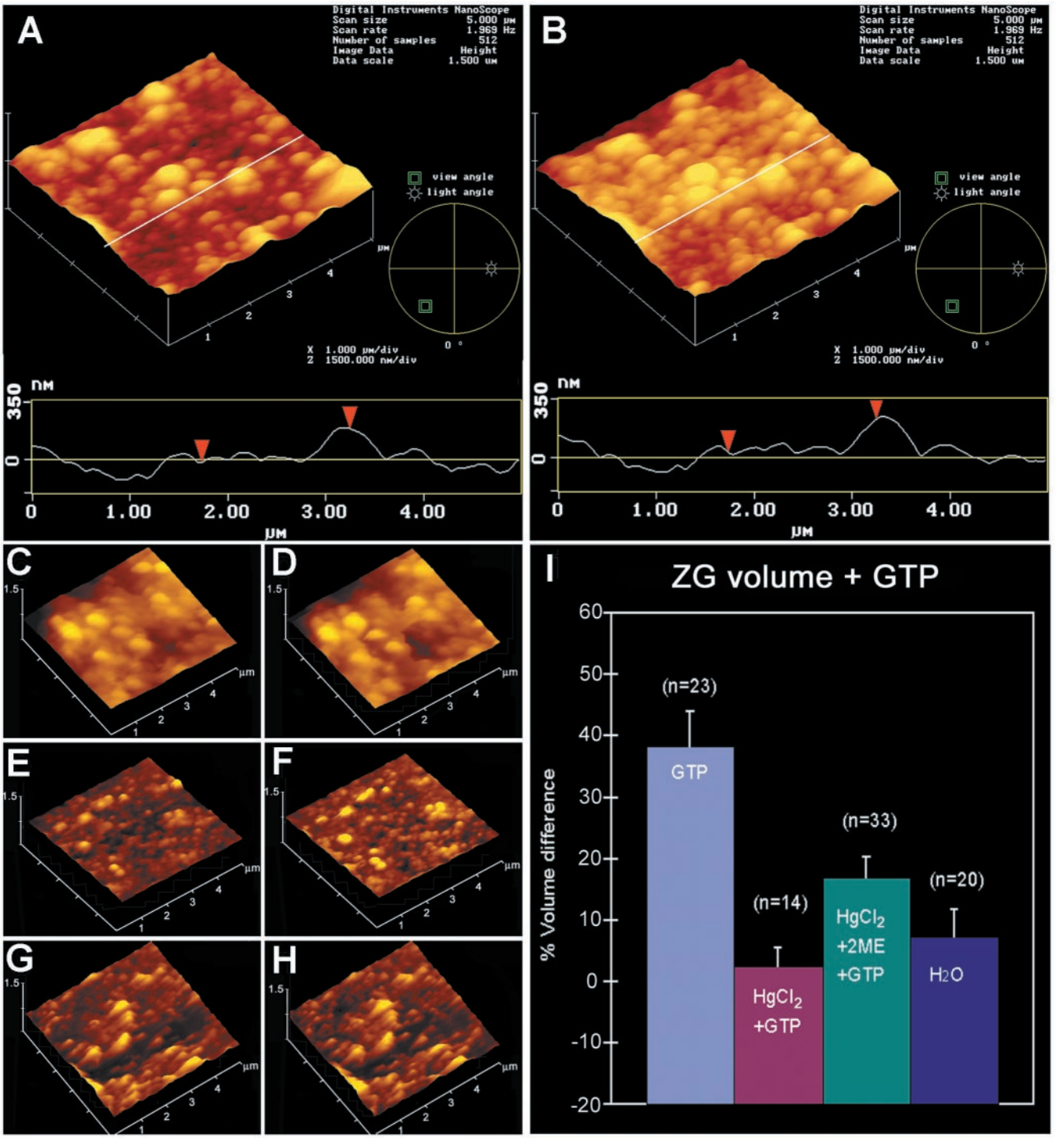

Fig. 3. Sensitivity of GTP-induced ZG swelling. (*A–H*) Three-dimensional atomic force microscopy images and section analysis of ZG untreated (*A* and *B*) or pretreated with 25 μM $HgCl_2$ (*C* and *D*), pretreated with 25 μM $HgCl_2$ followed by 100 μM 2-mercaptoethanol (*E* and *F*), before (*A*, *C*, and *E*) and after (*B*, *D*, and *F*) exposure to 40 μM GTP. Notice the increase in size of ZG (from *A* to *B* and *I*) in the three-dimensional array, section analysis, and bar graph after exposure to GTP. Pretreatment of ZG with $HgCl_2$ abolishes the GTP effect (from *C* to *D* and *I*). However, the inhibitory effect of $HgCl_2$ is reversed partially in the presence of 2-mercaptoethanol (from *E* to *F* and *I*). Incubation of ZG in water instead of 125 mM KCl-Mes buffer, pH 6.5, has little effect on ZG size [time 0 min (*G*) to time 30 min (*H* and *I*).]

were exposed to different stimulators, inhibitors, or their respective controls. The reaction mixture was incubated at room temperature for 30 min, ZGs were collected by centrifugation, and tritiated water incorporation into them was estimated by liquid scintillation counting.

Results and Discussion

Water-Channel AQP1 at ZG Membrane. Pancreatic subcellular fractions (9, 10, 12–15, 23) demonstrate the presence of AQP1 immunoreactivity in ZG membrane preparations (Fig. 1*A*). A strong, immunoreactive signal also was observed in the pan-

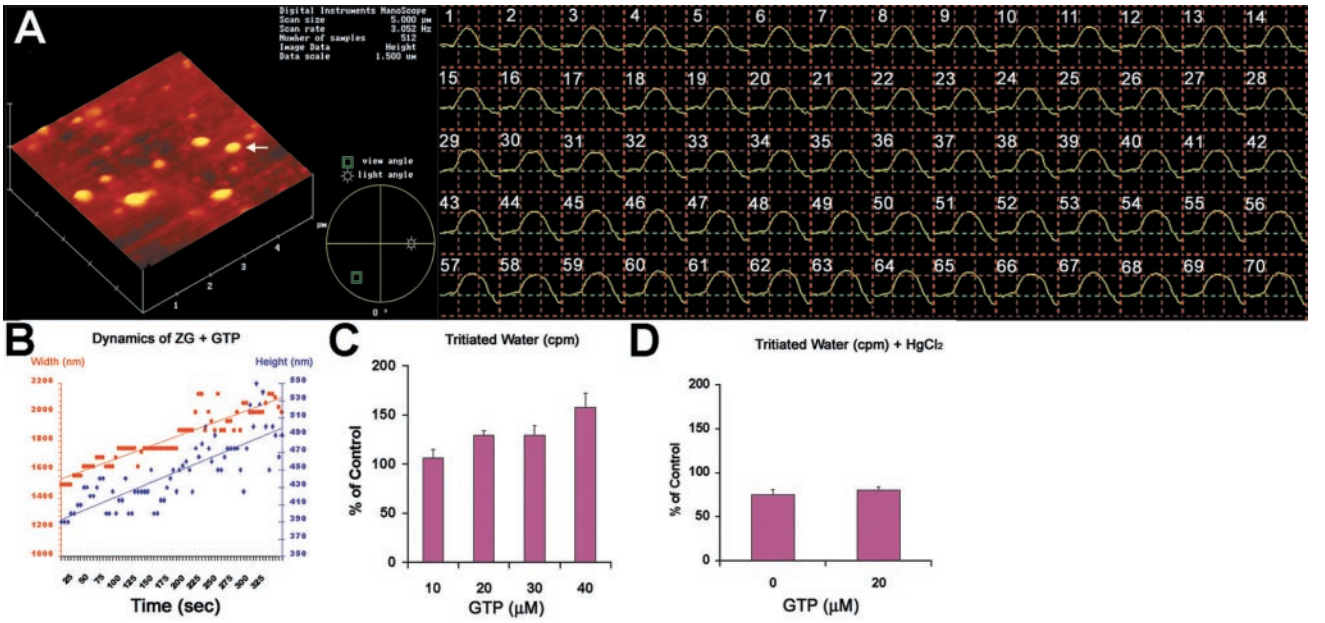

Fig. 4. GTP-induced ZG swelling is rapid and involves $HgCl_2$-sensitive ^3H_2O entry. (*A* and *B*) The height and width of a single ZG (yellow arrow) is monitored in seconds after exposure to 40 μM GTP. Notice the linear time-dependent increase in both height and width of the ZG after exposure to GTP. (*C*) A GTP-dose dependent increase in tritiated water entry is observed in ZG. (*D*) Exposure of ZG to $HgCl_2$ inhibits both basal and GTP-induced tritiated water entry into ZG.

creatic particulate fraction. Because it is possible for ZG to have been contaminated with other subcellular components enriched in AQP1, it was necessary to determine the purity of the ZG preparation. The purity of ZG and the ZG membrane fractions was determined by the enriched presence of VAMP immunoreactivity (Fig. 1*B*). VAMP, also known as synaptobrevin, is a VAMP present in ZG membranes. A significant enrichment of VAMP immunoreactivity was observed in ZG membrane, compared with other pancreatic fractions. To determine the type of association of AQP1 with ZGs, the ZG membrane was treated with salt (1 M KCl) and a nonionic detergent (1% Triton X-100). Detergent treatment released the AQP1 immunoreactivity from ZG membranes, but salt had no effect (Fig. 1*C*). These results show that AQP1, as its structure suggests (27, 28), is tightly associated with the ZG membrane. To determine the distribution of AQP1 in pancreatic acinar cells, AQP1 immunoreactivity was examined (29) by using both light (Fig. 2 *A–D*) and electron microscopy (Fig. 2*E*). Pancreatic acinar cells are polarized secretory cells that contain apically located ZGs. Abundant AQP1 immunoreactivity was detected at the apical region of these cells. In resting acini (Fig. 2 *A–D*), AQP1 immunoreactivity was detectable throughout the cell, but its primary localization was at the apical region. Electron microscopy confirmed the presence of AQP1 at the ZG membrane (Fig. 2*E*). It is well established that, after a secretory stimulus, there is release of granular contents at the apical lumen of pancreatic acini. Immunocytochemistry performed with light microscopy demonstrated intense, AQP1-specific labeling at the apical region of the cell (Fig. 2 *B* and *D*), suggesting the involvement of AQP1 in secretion.

GTP-Induced ZG Swelling Is $HgCl_2$-Sensitive. As demonstrated previously (22), exposure to GTP resulted in swelling (percent volume increase = 38.22 ± 5.87; mean ± SE) of isolated ZG preparations (Figs. 3 *A*, *B*, and *I* and 4 *A–C*). After exposure to 40 μM GTP, a marked increase in water entry into ZG was demonstrated within seconds (Fig. 4 *A* and *B*). Water permeability of ZG was GTP dose-dependent, assayed by the entry of tritiated water (Fig. 4*C*). The increased entry of tritiated water was 6.5% above control in the presence of 10 μM GTP, 29.6% in 20 μM GTP, and 58% in 40 μM GTP. However, exposure of

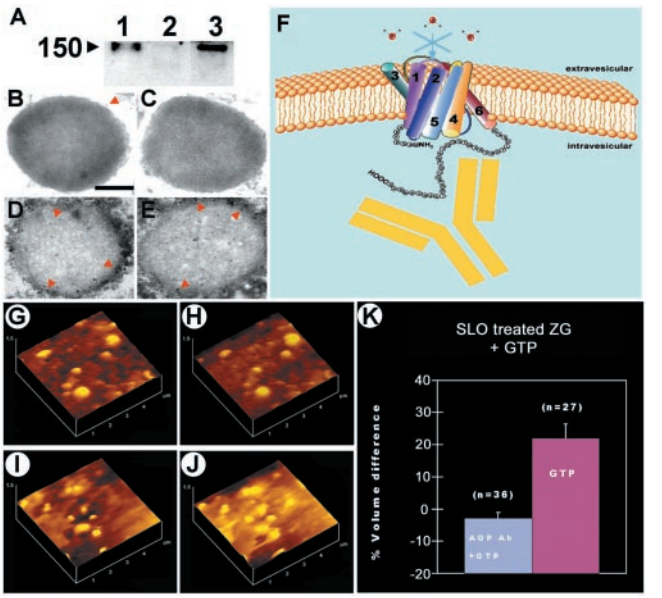

Fig. 5. AQP1-specific antibody binds to the ZG membrane and blocks water traffic. (*A*) Immunoblot assay demonstrating the presence of AQP1 antibody in SLO-permeabilized ZG. Lanes: 1, AQP1 antibody alone; 2, nonpermeable ZG exposed to antibody; 3, permeable ZG exposed to AQP1 antibody. Immunoelectron micrographs of intact ZGs exposed to AQP1 antibody demonstrate little labeling (*B* and *C*). (Bar = 200 nm.) Contrarily, SLO-treated ZG demonstrate intense gold labeling at the luminal side of the ZG membrane (*D* and *E*). AQP1 regulates GTP-induced water entry in ZG. (*F*) Schematic diagram of ZG membrane depicting AQP1-specific antibody binding to the carboxyl domain of AQP1 at the intragranular side to block water gating. (*G*, *H*, and *K*) AQP1 antibody introduced into ZG blocks GTP-induced water entry and swelling (from *G* to *H*, after GTP exposure). (*I–K*) However, only vehicle introduced into ZG retains the GTP-stimulatable effect (from *I* to *J*, after GTP exposure).

PHYSIOLOGY

ZG to $HgCl_2$, a known inhibitor of AQP1 (16, 17), resulted in inhibition of both the basal (75.1 ± 6.17% of control) as well as the GTP-mediated (80.43 ± 3.55% of control) water permeability (Figs. 3 *C*, *D*, and *I* and 4*D*). The effect of $HgCl_2$ on ZG was reversed by the presence of 1 mM 2-mercaptoethanol (Fig. 3 *E*, *F*, and *I*), as demonstrated by a 16.83 ± 3.53% GTP-induced increase in the volume of $HgCl_2$-treated vesicles after exposure to 1 mM 2-mercaptoethanol.

Functional AQP1 at ZG Membrane. To determine whether the GTP-induced water entry was a result of AQP1 water-channel function or osmosis-driven, isolated ZGs were incubated in water and their size was monitored. Isolated ZG incubated in water had little effect (Fig. 3 *G*, *H*, and *I*), as shown by no significant change in ZG volume over control (7.32 ± 4.51%). The presence of functional AQP1 in ZG membranes was confirmed from tritiated water-permeability experiments on isolated ZG. ZGs were incubated in buffer containing ^3H_2O in the presence and absence of GTP and/or $HgCl_2$. GTP is known to induce swelling of isolated ZGs (22). Exposure of isolated ZGs to GTP (10–40 μM) resulted in an increase in water entry in a dose-dependent manner (Fig. 4*C*). In the presence of $HgCl_2$, GTP-induced water entry was inhibited (Fig. 4*D*). Isolated ZGs were stable for hours in low pH (pH 6–6.5) buffers. At neutral or alkaline pH, isolated ZGs rapidly lysed. All studies therefore were performed in pH 6.5 buffer. These results, however, do not exclude the possibility that yet unidentified mercury-sensitive water channels may contribute to GTP-stimulatable water entry into ZGs. This issue was addressed by introducing AQP1-specific antibody raised against the carboxyl domain of the water channel into ZGs.

AQP1 Regulates ZG Swelling. The introduction of AQP1-specific antibody into isolated ZG was carried out by permeabilizing ZG with SLO. We next carried out an experiment to determine whether the AQP1 antibody actually entered the SLO-treated ZGs and, if so, their distribution within the ZG. Both Western blot assay and immunoelectron microscopy demonstrated the entry of AQP1 antibody into ZGs (Fig. 5 *A–E*). When intact and permeabilized ZGs were exposed separately to the AQP1 antibody, resolved using SDS/PAGE, followed by transfer to nitrocellular membrane, and probed using a secondary antibody conjugated to a chemiluminescent marker, the AQP antibody was detected in the SLO-treated ZG. This demonstrated entry of the antibody in SLO-treated ZG. No detectable signal was seen in the intact ZG fraction exposed to the AQP1 antibody (Fig. 5*A*). Electron microscopy performed in the intact and SLO-treated ZG demonstrated intense immunogold localization in the SLO-treated ZGs, confirming AQP1 entry into the ZGs. Specific immunogold-labeling at the luminal side of the ZG membrane in the SLO-treated batch further confirms binding of the antibody to the carboxyl domain of AQP1. When AQP1-specific antibody was introduced into SLO-permeabilized ZGs (Fig. 5 *A–F*), GTP-induced water entry was inhibited (Fig. 5 *G*, *H*, and *K*). However, in the absence of AQP1-specific antibody, SLO-permeabilized ZGs elicit strong, GTP-induced swelling (volume increase of 21.95 ± 4.42%; Fig. 5 *I–K*). These studies demonstrate that at pH 6.5, AQP1 participates in GTP-induced gating of water in ZG of pancreatic acinar cells. Previous studies demonstrated that the carboxyl domain of AQP1 does not participate in water entry (30). However, the inhibition of AQP1 by the antibody may result from the structural distortion of AQP1 by binding of the comparatively larger antibody molecule. To understand the detailed pathway of GTP-induced signaling in the regulation of AQP1 in ZG membrane, further studies are required. Studies using liposomes reconstituted with AQP1, the $G_{\alpha i3}$ protein, and other signaling molecules will help elucidate the molecular mechanism of GTP-induced and AQP1-mediated water entry into ZG. It is likely, however, that the effect of GTP on the regulation of AQP1 may not be direct.

We thank Peter Agre for reading this manuscript and for his valuable comments and suggestions. This work was supported in part by National Institutes of Health Grants DK56212 and NS39918 (to B.P.J.). S.J.C. is a recipient of a National Institutes of Health postdoctoral fellowship award (DK60368).

1. Alvarez de Toledo, G., Fernandez-Chacon, R. & Fernandez, J. M. (1993) *Nature (London)* **363,** 554–558.
2. Curran, M. J. & Brodwick, M. S. (1991) *J. Gen. Physiol.* **98,** 771–790.
3. Monck, J. R., Oberhauser, A. F., Alvarez de Toledo, G. & Fernandez, J. M. (1991) *Biophys. J.* **59,** 39–47.
4. Finkelstein, A., Zimmerberg, J. & Cohen, F. S. (1986) *Annu. Rev. Physiol.* **48,** 163–174.
5. Fernandez, J. M., Villalon, M. & Verdugo, P. (1991) *Biophys. J.* **59,** 1022–1027.
6. Gasser, K. W., DiDomenico, J. & Hopfer, U. (1988) *Am. J. Physiol.* **254,** G93–G99.
7. Yasui, M., Hazama, A., Kwon, T. H., Nielsen, S., Guggino, W. B. & Agre, P. (1999) *Nature (London)* **402,** 184–187.
8. Marinelli, R. A., Pham, L., Agre, P. & LaRusso, N. F. (1997) *J. Biol. Chem.* **272,** 12984–12988.
9. Delporte, C., O'Connell, B. C., He, X., Lancaster, H. E., O'Connell, A. C., Agre, P. & Baum, B. J. (1997) *Proc. Natl. Acad. Sci. USA* **94,** 3268–3273.
10. Knepper, M. A. & Inoue, T. (1997) *Curr. Opin. Cell Biol.* **9,** 560–564.
11. Knepper, M. A. (1994) *Proc. Natl. Acad. Sci. USA* **91,** 6255–6258.
12. Jena, B. P., Padfield, P. J., Ingebritsen, T. S. & Jamieson, J. D. (1991) *J. Biol. Chem.* **266,** 17744–17746.
13. Cameron, R. S., Cameron, P. L. & Castle, J. D. (1986) *J. Cell Biol.* **103,** 1299–1313.
14. Bradford, M. M. (1976) *Anal. Biochem.* **72,** 248–254.
15. Laemmli, U. K. (1970) *Nature (London)* **227,** 680–685.
16. Agre, P., Bonhivers, M. & Borgnia, M. J. (1998) *J. Biol. Chem.* **273,** 14659–14662.
17. Preston, G. M., Carroll, T. P., Guggino, W. B. & Agre, P. (1992) *Science* **256,** 385–387.
18. Ito, H., Tung, R. T., Sugimoto, T., Kobayashi, I., Takahashi, K., Katada, T., Ui, M. & Kurachi, Y. (1992) *J. Gen. Physiol.* **99,** 961–983.
19. Schwiebert, E. M., Kizer, N., Gruenert, D. C. & Stanton, B. A. (1992) *Proc. Natl. Acad. Sci. USA* **89,** 10623–10627.
20. Kirsch, G. E., Codina, J., Birnbaumer, L. & Brown, A. M. (1990) *J. Am. Physiol.* **259,** H820–H826.
21. Schwiebert, E. M., Light, D. B., Fejes-Toth, G., Naray-Fejes-Toth, A. & Stanton, B. A. (1990) *J. Biol. Chem.* **265,** 7725–7728.
22. Jena, B. P. Schneider, S. W., Geibel, J. P., Webster, P., Oberleithner, H. & Sritharan, K. C. (1997) *Proc. Natl. Acad. Sci. USA* **94,** 13317–13322.
23. Rosenzweig, S. A., Miller, L. J. & Jamieson, J. D. (1983) *J. Cell Biol.* **96,** 1288–1297.
24. Bendayan, M. (1984) *J. Electron Microsc. Tech.* **1,** 243–270.
25. Schneider, S. W., Sritharan, K. C., Geibel, J. P., Oberleithner, H. & Jena, B. P. (1997) *Proc. Natl. Acad. Sci. USA* **94,** 316–321.
26. Henderson, R. M., Schneider, S., Li, Q., Hornby, D., White, S. J. & Oberleithner, H. (1996) *Proc. Natl. Acad. Sci. USA* **93,** 8756–8760.
27. Walz, T., Hirai, T., Murata, K., Heymann, J. B., Mitsuoka, K., Fujiyoshi, Y., Smith, B. L., Agre, P. & Engel, A. (1997) *Nature (London)* **387,** 624–627.
28. Cheng, A., van Hoek, A. N., Yeager, M., Verkman, A. S. & Mitra, A. K. (1997) *Nature (London)* **387,** 627–630.
29. Jena, B. P., Gumkowski, F. D., Konieczko, E. M., von Mollard, G. F., Jahn, R. & Jamieson, J. D. (1994) *J. Cell Biol.* **124,** 43–53.
30. Murata, K., Mitsuoka, K., Hirai, T., Walz, T., Agre, P., Heymann, J. B., Engel, A. & Fujiyoshi, Y. (2000) *Nature (London)* **407,** 599–605.